The Astrophysical Journal, 920:50 (6pp), 2021 October 10 https://doi.org/10.3847/1538-4357/ac16d6

Search for Neutrinos from the Tidal Disruption Events AT2019dsg and AT2019fdr with the ANTARES Telescope

A. Albert[1,2], S. Alves[3], M. André[4], M. Anghinolfi[5], G. Anton[6], M. Ardid[7], J.-J. Aubert[8], J. Aublin[9], B. Baret[9], S. Basa[10], B. Belhorma[11], M. Bendahman[9,12], F. Benfenati[13,14], V. Bertin[8], S. Biagi[15], M. Bissinger[6], J. Boumaaza[12], M. Bouta[16], M. C. Bouwhuis[17], H. Brânzaş[18], R. Bruijn[17,19], J. Brunner[8], J. Busto[8], B. Caiffi[5], A. Capone[20,21], L. Caramete[18], J. Carr[8], V. Carretero[3], S. Celli[20,21], M. Chabab[22], T. N. Chau[9], R. Cherkaoui El Moursli[12], T. Chiarusi[13], M. Circella[23], A. Coleiro[9], M. Colomer-Molla[3,9], R. Coniglione[15], P. Coyle[8], A. Creusot[9], A. F. Díaz[24], G. de Wasseige[9], A. Deschamps[25], C. Distefano[15], I. Di Palma[20,21], A. Domi[5,26], C. Donzaud[9,27], D. Dornic[8], D. Drouhin[1,2], T. Eberl[6], T. van Eeden[17], N. El Khayati[12], A. Enzenhöfer[8], P. Fermani[20,21], G. Ferrara[15], F. Filippini[13,14], L. Fusco[8], R. García[17], Y. Gatelet[9], P. Gay[9,28], H. Glotin[29], R. Gozzini[6], K. Graf[6], C. Guidi[5,26], S. Hallmann[6], H. van Haren[30], A. J. Heijboer[17], Y. Hello[25], J. J. Hernández-Rey[3], J. Hößl[6], J. Hofestädt[6], F. Huang[1], G. Illuminati[9,13,14], C. W. James[31], B. Jisse-Jung[17], M. de Jong[17,32], P. de Jong[17], M. Jongen[17], M. Kadler[33], O. Kalekin[6], U. Katz[6], N. R. Khan-Chowdhury[3], A. Kouchner[9], I. Kreykenbohm[34], V. Kulikovskiy[5], R. Lahmann[6], R. Le Breton[9], D. Lefèvre[35], E. Leonora[36], G. Levi[13,14], M. Lincetto[8], D. Lopez-Coto[37], S. Loucatos[9,38], L. Maderer[9], J. Manczak[3], M. Marcelin[10], A. Margiotta[13,14], A. Marinelli[39], J. A. Martínez-Mora[7], K. Melis[17,19], P. Migliozzi[39], M. Moser[6], A. Moussa[16], R. Muller[17], L. Nauta[17], S. Navas[37], E. Nezri[10], B. Ó Fearraigh[17], M. Organokov[1], G. E. Păvălaş[18], C. Pellegrino[13,40,41], M. Perrin-Terrin[8], P. Piattelli[15], C. Pieterse[3], C. Poirè[7], V. Popa[18], T. Pradier[1], N. Randazzo[36], S. Reck[6], G. Riccobene[15], A. Romanov[5], F. Salesa Greus[3], D. F. E. Samtleben[17,32], A. Sánchez-Losa[23], M. Sanguineti[5,26], P. Sapienza[15], J. Schnabel[6], J. Schumann[6], F. Schüssler[38], M. Spurio[13,14], Th. Stolarczyk[38], M. Taiuti[5,26], Y. Tayalati[12], S. J. Tingay[31], B. Vallage[9,38], V. Van Elewyck[9,42], F. Versari[9,13,14], S. Viola[15], D. Vivolo[39,43], J. Wilms[34], S. Zavatarelli[5], A. Zegarelli[20,21], J. D. Zornoza[3], and J. Zúñiga[3]

(ANTARES Collaboration)

[1] Université de Strasbourg, CNRS, IPHC UMR 7178, F-67000 Strasbourg, France
[2] Université de Haute Alsace, F-68200 Mulhouse, France
[3] IFIC—Instituto de Física Corpuscular (CSIC—Universitat de València) c/ Catedrático José Beltrán, 2 E-46980 Paterna, Valencia, Spain
[4] Technical University of Catalonia, Laboratory of Applied Bioacoustics, Rambla Exposició, E-08800 Vilanova i la Geltrú, Barcelona, Spain
[5] INFN—Sezione di Genova, Via Dodecaneso 33, I-16146 Genova, Italy
[6] Friedrich-Alexander-Universität Erlangen-Nürnberg, Erlangen Centre for Astroparticle Physics, Erwin-Rommel-Str. 1, D-91058 Erlangen, Germany
[7] Institut d'Investigació per a la Gestió Integrada de les Zones Costaneres (IGIC) - Universitat Politècnica de València, C/ Paranimf 1, E-46730 Gandia, Spain
[8] Aix Marseille Université, CNRS/IN2P3, CPPM, Marseille, France
[9] Université de Paris, CNRS, Astroparticule et Cosmologie, F-75006 Paris, France
[10] Aix Marseille Université, CNRS, CNES, LAM, Marseille, France
[11] National Center for Energy Sciences and Nuclear Techniques, B.P.1382, R.P.10001 Rabat, Morocco
[12] University Mohammed V in Rabat, Faculty of Sciences, 4 av. Ibn Battouta, B.P. 1014, R.P. 10000, Morocco
[13] INFN—Sezione di Bologna, Viale Berti-Pichat 6/2, I-40127 Bologna, Italy
[14] Dipartimento di Fisica e Astronomia dell'Università, Viale Berti Pichat 6/2, I-40127 Bologna, Italy; giulia.illuminati3@unibo.it
[15] INFN—Laboratori Nazionali del Sud (LNS), Via S. Sofia 62, I-95123 Catania, Italy
[16] University Mohammed I, Laboratory of Physics of Matter and Radiations, B.P.717, Oujda 6000, Morocco
[17] Nikhef, Science Park, Amsterdam, The Netherlands
[18] Institute of Space Science, RO-077125 Bucharest, Măgurele, Romania
[19] Universiteit van Amsterdam, Instituut voor Hoge-Energie Fysica, Science Park 105, 1098 XG Amsterdam, The Netherlands
[20] INFN—Sezione di Roma, P.le Aldo Moro 2, I-00185 Roma, Italy
[21] Dipartimento di Fisica dell'Università La Sapienza, P.le Aldo Moro 2, I-00185 Roma, Italy
[22] LPHEA, Faculty of Science—Semlali, Cadi Ayyad University, P.O.B. 2390, Marrakech, Morocco
[23] INFN—Sezione di Bari, Via E. Orabona 4, I-70126 Bari, Italy
[24] Department of Computer Architecture and Technology/CITIC, University of Granada, E-18071 Granada, Spain
[25] Géoazur, UCA, CNRS, IRD, Observatoire de la Côte d'Azur, Sophia Antipolis, France
[26] Dipartimento di Fisica dell'Università, Via Dodecaneso 33, I-16146 Genova, Italy
[27] Université Paris-Sud, F-91405 Orsay Cedex, France
[28] Laboratoire de Physique Corpusculaire, Clermont Université, Université Blaise Pascal, CNRS/IN2P3, BP 10448, F-63000 Clermont-Ferrand, France
[29] LIS, UMR Université de Toulon, Aix Marseille Université, CNRS, F-83041 Toulon, France
[30] Royal Netherlands Institute for Sea Research (NIOZ), Landsdiep 4, 1797 SZ 't Horntje (Texel), The Netherlands
[31] International Centre for Radio Astronomy Research—Curtin University, Bentley, WA 6102, Australia
[32] Huygens-Kamerlingh Onnes Laboratorium, Universiteit Leiden, The Netherlands
[33] Institut für Theoretische Physik und Astrophysik, Universität Würzburg, Emil-Fischer Str. 31, D-97074 Würzburg, Germany
[34] Dr. Remeis-Sternwarte and ECAP, Friedrich-Alexander-Universität Erlangen-Nürnberg, Sternwartstr. 7, D-96049 Bamberg, Germany
[35] Mediterranean Institute of Oceanography (MIO), Aix-Marseille University, F-13288, Marseille, Cedex 9, France; Université du Sud Toulon-Var, CNRS-INSU/IRD UM 110, F-83957, La Garde Cedex, France
[36] INFN—Sezione di Catania, Via S. Sofia 64, I-95123 Catania, Italy
[37] Dpto. de Física Teórica y del Cosmos & C.A.F.P.E., University of Granada, E-18071 Granada, Spain
[38] IRFU, CEA, Université Paris-Saclay, F-91191 Gif-sur-Yvette, France
[39] INFN—Sezione di Napoli, Via Cintia I-80126 Napoli, Italy
[40] Museo Storico della Fisica e Centro Studi e Ricerche Enrico Fermi, Piazza del Viminale 1, I-00184, Roma, Italy
[41] INFN—CNAF, Viale C. Berti Pichat 6/2, I-40127, Bologna, Italy
[42] Institut Universitaire de France, F-75005 Paris, France

[43] Dipartimento di Fisica dell'Università Federico II di Napoli, Via Cintia I-80126, Napoli, Italy
Received 2021 March 31; revised 2021 July 7; accepted 2021 July 20; published 2021 October 12

Abstract

On 2019 October 1, the IceCube Collaboration detected a muon track neutrino with a high probability of being of astrophysical origin, IC191001A. After a few hours, the tidal disruption event (TDE) AT2019dsg, observed by the Zwicky Transient Facility (ZTF), was indicated as the most likely counterpart of the IceCube track. More recently, the follow-up campaign of the IceCube alerts by ZTF suggested a second TDE, AT2019fdr, as a promising counterpart of another IceCube muon track candidate, IC200530A, detected on 2020 May 30. Here, these intriguing associations are followed-up by searching for neutrinos in the ANTARES detector from the directions of AT2019dsg and AT2019fdr using a time-integrated approach. As no significant evidence for space clustering is found in the ANTARES data, upper limits on the one-flavor neutrino flux and fluence are set.

Unified Astronomy Thesaurus concepts: Neutrino astronomy (1100)

1. Introduction

High-energy cosmic neutrinos are a unique probe of the high-energy universe: their detection is critical to identify the acceleration sites of cosmic rays and to discover distant sources otherwise inaccessible with γ-rays. Several milestones have been achieved in the field of neutrino astronomy in the past decade, which also opened new unresolved questions.

The IceCube Collaboration has detected an isotropic high-energy cosmic neutrino flux with a high level of significance in several diffuse flux searches (Aartsen et al. 2014, 2016). A mild excess, consistent with the IceCube findings, has also been seen in the ANTARES data (Albert et al. 2018a). However, the sources responsible for the diffuse cosmic signal have not been yet identified.

In 2017, an event observed in the IceCube detector induced by a ∼300 TeV muon neutrino was found positionally coincident with the direction of a known blazar in a flaring state, TXS 0506+056 (Kopper & Blaufuss 2017; Aartsen et al. 2018a). Soon after, the IceCube Collaboration reported compelling evidence for an earlier neutrino flare from the same direction found in the archival data (Aartsen et al. 2018b). This led to the first association of high-energy neutrinos with an astrophysical source at the 3 σlevel. However, the expected neutrino emission from the blazar TXS 0506+056 can only contribute to the IceCube cosmic neutrino flux for less than 1% (Aartsen et al. 2018b). The region around TXS 0506+056 was studied also by the ANTARES Collaboration, yielding no significant correlation in time and/or space with the IceCube neutrinos (Albert et al. 2018b).

In 2020, a new likely association between an IceCube neutrino, IC191001A, and an astrophysical source, the tidal disruption event (TDE) AT2019dsg, was announced (Stein et al. 2021). Soon after, a second TDE, ZTF19aatubsj/AT2019fdr (hereafter referred to as AT2019fdr), was found positionally coincident with another IceCube neutrino, IC200530A (Reusch 2020). TDEs are rare transient phenomena that occur when a star passes close enough to a supermassive black hole and is disrupted by the strong tidal forces (for recent reviews see Lodato et al. 2015; Komossa 2015). The accretion process onto the black hole involves about half of the stellar mass and, in some cases, results in a relativistic jet. Consequently, both jetted and nonjetted TDEs are observed. Since TDEs show nonthermal radio emission, they have been suggested as promising sources of ultra-high energy cosmic rays and high-energy neutrinos (see Biehl et al. 2018 and references therein). Nonetheless, the contribution to the IceCube diffuse flux from the TDEs detected before AT2019dsg and AT2019fdr has been constrained to be at most ∼1.3% (∼26%) in the jetted (nonjetted) TDE case (Stein 2020).

The detection of IC191001A, a ∼200 TeV muon neutrino with 59% probability of being of astrophysical origin, registered by IceCube on 2019 October 1 (https://gcn.gsfc.nasa.gov/amon_icecube_gold_bronze_events.html; Stein 2019), triggered dedicated follow-ups by multiple telescopes, including the Zwicky Transient Facility (ZTF; Bellm et al. 2018; Graham et al. 2019). While several optical transients were found within the 90% localization uncertainty of the neutrino direction (∼26 deg^2) by ZTF, the TDE AT2019dsg, being one of the few ever detected radio-emitting TDEs, was soon identified as the most promising candidate neutrino source (Stein 2019; Stein et al. 2021). Analogously, IC200530A,a ∼80 TeV muon neutrino with a 59% probability of being of astrophysical origin, detected by IceCube on 2020 May 30 (AMON IceCube Gold and Bronze Event Information; Stein 2020b), was followed by ZTF, which indicated AT2019fdr as the likely counterpart of the neutrino event (Reusch 2020).

AT2019dsg and AT2019fdr were first discovered by ZTF on 2019 April 9 (Nordin et al. 2019) and on 2019 April 27 (Frederick et al. 2020), respectively. The TDEs showed a luminosity peak in the optical/UV bands, and appeared to have reached a luminosity plateau by the time of the neutrino detections, which happened ∼150 days and about one year after the peak, respectively (Frederick et al. 2020; Stein et al. 2021). As detailed in Stein et al. (2021), after the discovery, AT2019dsg was also detected in several follow-up observations in optical/UV, X-rays, and radio, indicating particle acceleration to relativistic energies. The probability of finding by chance a radio-emitting TDE as bright as AT2019dsg in bolometric energy flux and in coincidence with the IceCube neutrino was estimated to be 0.2%. The expected neutrino flux from AT2019dsg has been calculated for different models of multimessenger emission both in the jetted (Liu et al. 2020; Winter & Lunardini 2021) and nonjetted (Murase et al. 2020) TDE cases. The most optimistic scenarios predict a neutrino fluence of $\sim 10^{-2}$ GeV cm^{-2}.

In this article, the ANTARES follow-up of these findings is presented. In particular, the ANTARES data collected since the discovery of AT2019dsg and AT2019fdr are investigated to look for a steady neutrino emission from the direction of the TDEs.

2. Detector and Data Sample

The ANTARES neutrino telescope (Ageron et al. 2011) is a three-dimensional array of 885 photomultiplier tubes (PMTs) located 40 km off-shore from Toulon, France, below the surface of the Mediterranean Sea. The 10 inch PMTs are distributed along 12, 450 m long, vertical lines anchored to the seabed at a depth of about 2500 m and held taut by a buoy at the top, instrumenting a total volume of $\sim 0.01\,\mathrm{km}^3$. The neutrino detection principle is based on the collection of the Cerenkov light induced by relativistic charged particles, which are produced in neutrino interactions within and around the instrumented volume. The information provided by the position, time, and collected charge of the signals in the PMTs is used to infer the direction and energy of the incident neutrino.

Different neutrino flavors and interactions leave distinct signatures in the detector. Two event topologies can be identified in the ANTARES telescope: tracks and showers. Tracks are originated by the passage in water of relativistic muons produced in charged current (CC) interactions of muon neutrinos. The long lever arm of the track topology allows us to reconstruct the parent neutrino direction of high-quality selected events with a median angular resolution of $\sim 0.^{\circ}8$ at $E_\nu \sim 1$ TeV and below $\sim 0.^{\circ}4$ for $E_\nu > 10$ TeV (Albert et al. 2017). All-flavor neutral current (NC) as well as ν_e and ν_τ CC interactions induce showers, characterized by an almost spherical light emission around the shower maximum, with an elongation of a few meters. A median angular resolution of $\sim 3^{\circ}$ for high-quality selected events with E_ν between 1 TeV and 0.5 PeV is achieved for this topology (Albert et al. 2017).

The search for neutrinos from the direction of AT2019dsg (AT2019fdr) presented in this article includes both track-like and shower-like events. Given the late IceCube neutrino detection with respect to the TDE luminosity peak, the events recorded in ANTARES from the day of the discovery of the TDE, 2019 April 9 (2019 April 27), until the day of the last available fully calibrated ANTARES data, 2020 February 29, are employed in the search, for a total livetime of 315 (298) days. The model presented in Winter & Lunardini (2021) shows that neutrino emission can still be expected after ~ 300 days from the TDE luminosity peak. The track and shower events are selected using the criteria described in Albert et al. (2017). The selection is optimized to minimize the neutrino flux needed for a $5\,\sigma$ discovery of a point-like source emitting with an energy spectrum of $\propto E_\nu^{-2.0}$. Cuts are applied on the zenith angle, the angular error estimate and parameters describing the quality of the reconstruction. In the shower channel, an additional cut is applied on the interaction vertex, required to be located within a fiducial volume slightly larger than the instrumented volume. A total of 413 (390) tracks and 8 (7) showers, resulting from the selection, are employed in the search for a cluster of events from the direction of AT2019dsg (AT2019fdr).

3. Search Method

The location of AT2019dsg (R. A. $= 314.^{\circ}26$, $\delta = 14.^{\circ}20$) and of AT2019fdr (R. A. $= 257.^{\circ}28$, $\delta = 26.^{\circ}86$) has been investigated to search for spatial clustering of events above the known background expectation following an unbinned maximum likelihood ratio approach. The likelihood describes the ANTARES data in terms of signal and background probability density functions (PDFs) and is defined as:

$$\log \mathcal{L} = \sum_{\mathcal{J}\in\{\mathrm{tr,sh}\}} \sum_{i\in\mathcal{J}} \log\left[\mu_{\mathrm{sig}}^{\mathcal{J}} \mathcal{S}_i^{\mathcal{J}} + \mathcal{N}^{\mathcal{J}} \mathcal{B}_i^{\mathcal{J}}\right] - \mu_{\mathrm{sig}}, \qquad (1)$$

where $\mathcal{S}_i^{\mathcal{J}}$ and $\mathcal{B}_i^{\mathcal{J}}$ are the values of the signal and background PDFs for the event i in the sample $\mathcal{J}$ (tr for tracks, sh for showers), $\mu_{\mathrm{sig}}^{\mathcal{J}}$ and $\mathcal{N}^{\mathcal{J}}$ are the number of unknown signal events and the total number of data events in the $\mathcal{J}$ sample, respectively, and $\mu_{\mathrm{sig}} = \mu_{\mathrm{sig}}^{\mathrm{tr}} + \mu_{\mathrm{sig}}^{\mathrm{sh}}$ is the total number of fitted signal events. The PDFs have been built using the 2007-2020 ANTARES data and Monte Carlo production in order to ensure sufficient statistics. The signal and background PDFs are given by the product of a directional and an energy-dependent term. While atmospheric neutrino events appear randomly distributed on the sky, neutrinos from point-like sources are expected to accumulate around the source position. The energy information helps to distinguish signal from background, as a softer energy spectrum is predicted for atmospheric neutrinos with respect to the expected signal (Albert et al. 2021). An unbroken power-law neutrino spectrum, $\Phi_\nu(E_\nu) \propto E_\nu^{-\gamma}$, is assumed in this analysis for the signal emission, with γ being one of the three tested spectral indices, $\gamma = 2.0$, $\gamma = 2.5$, or $\gamma = 3.0$. The same definition of the PDFs used in the ANTARES 9 yr point-source analysis (Albert et al. 2017) is employed in this search. The spatial signal PDF is a spline parameterization of the point-spread function. It is defined as the PDF to reconstruct an event at a given angular distance from its original direction due to reconstruction uncertainties, and it is derived from Monte Carlo simulations of $\propto E_\nu^{-\gamma}$ cosmic neutrinos. The background is assumed to be uniform in R.A., and the distribution of the sine of the decl. of the selected data is employed as spatial background PDF. Monte Carlo simulations of $\propto E_\nu^{-\gamma}$ energy spectrum cosmic neutrinos (signal), assuming neutrino flavor equipartition at Earth and of atmospheric neutrinos using the spectrum of Barr et al. (2004; background), are used to derive the energy PDFs. In the likelihood maximization, the number of signal events, μ_{sig}, is the only free parameter. The test statistic, $\mathcal{Q}$, is defined from the likelihood as:

$$\mathcal{Q} = 2\log\left[\frac{\mathcal{L}(\mu_{\mathrm{sig}} = \hat{\mu}_{\mathrm{sig}})}{\mathcal{L}(\mu_{\mathrm{sig}} = 0)}\right], \qquad (2)$$

where $\hat{\mu}_{\mathrm{sig}}$ is the best-fit value that maximizes the likelihood. The significance of the potential spatial cluster at the location of the TDE is estimated by means of pseudo-experiments (PEs) —pseudo-data sets of data randomized in time to eliminate any local clustering due to potential sources. The fraction of background-only PEs with a value of $\mathcal{Q}$ larger than the one obtained with the data gives the significance (p-value) of the cluster.

The 5σ discovery potential of the search, $n^{5\,\sigma}$, is defined as the mean number of injected signal events needed for a 5σ discovery in 50% of the PEs. The obtained values are $n^{5\,\sigma} = 3.6$ and $n^{5\,\sigma} = 3.4$ for AT2019dsg and AT2019fdr, respectively, assuming an $E_\nu^{-2.0}$ neutrino spectrum, while $\sim 40\%$ more events are needed for the softer spectrum $E_\nu^{-3.0}$.

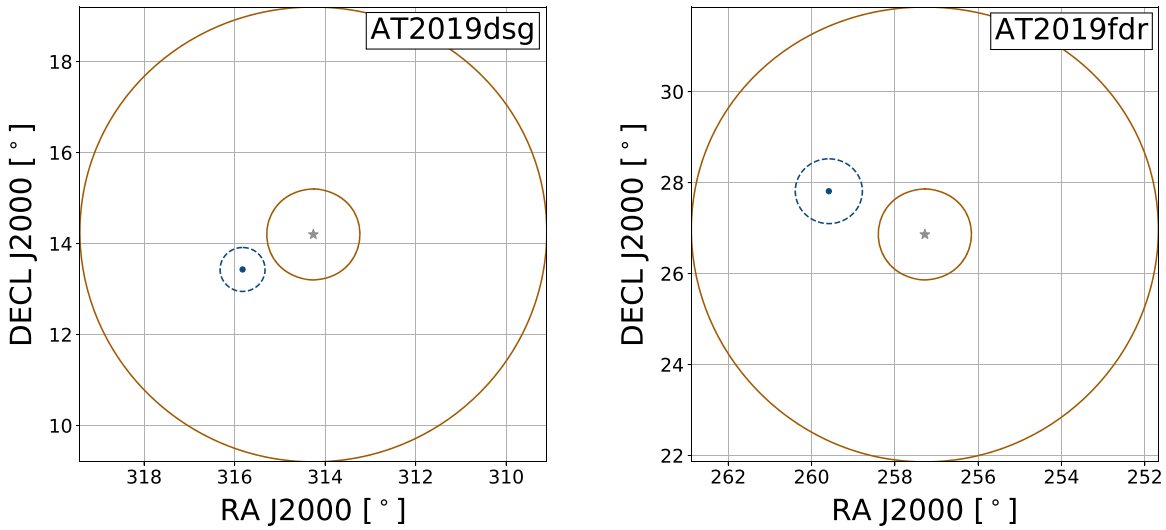

Figure 1. Distribution of ANTARES events in equatorial coordinates around the positions of AT2019dsg (left) and AT2019fdr (right). The orange lines depict the 1° and 5° distance from the source position, indicated as a gray star. Only track-like events (blue points) have been detected within 5° from the location of the sources. The dashed circles around the events indicate the angular error estimate on the track reconstructed direction.

Table 1
Neutrino Candidates Registered By the ANTARES Detector within an Angular Distance $\Delta\Psi$ from the TDEs

Source	Topology	(R.A., δ) (deg)	$\Delta\Psi$ (deg)	MJD	Date (dd/mm/year)	ΔT (days)	ff
AT2019dsg	track	(315.8, 13.4)	1.7	58890.99	11/02/2020	309	0.35
AT2019fdr	track	(259.6, 27.8)	2.3	58751.08	25/09/2019	151	0.15

Note. ANTARES event within an angular distance $\Delta\Psi < 5°$ from AT2019dsg (first row) and AT2019fdr (second row). For each ANTARES event, the table reports the topology, equatorial coordinates (R.A., δ), angular distance $\Delta\Psi$ from the TDE, Modified Julian Date (MJD), date (dd/mm/year), time distance ΔT between the event detection and the discovery of the TDE, and fraction ff of selected data events with energy estimator values larger than that of the event.

Table 2
Results of the Search at the Locations of AT2019dsg and AT2019fdr

Source		Results						
Name	γ	$\hat{\mu}_{\rm sig}$	p-value	$\Phi_0^{90\%\rm C.L.}$		$\mathcal{F}^{90\%\rm C.L.}$		$\log\left(\frac{E_{\rm min}}{\rm GeV}\right)$ - $\log\left(\frac{E_{\rm max}}{\rm GeV}\right)$
				Sensitivity	Limit	Sensitivity	Limit	
AT2019dsg	2.0	< 0.1	12.4%	7.3×10^{-8}	1.0×10^{-7}	14	19	3.6–6.6
	2.5	0.2	10.2%	1.5×10^{-5}	2.2×10^{-5}	29	43	2.8–5.5
	3.0	0.7	8.9%	1.2×10^{-3}	2.0×10^{-3}	230	380	2.1–4.7
AT2019fdr	2.0	0.5	6.7%	8.5×10^{-8}	1.3×10^{-7}	15	23	3.6–6.6
	2.5	0.5	7.9%	2.1×10^{-5}	3.0×10^{-5}	39	55	2.8–5.5
	3.0	0.6	9.1%	2.0×10^{-3}	3.0×10^{-3}	360	540	2.1–4.7

Note. Results of the search at the locations of AT2019dsg and AT2019fdr in terms of best-fit number of signal events $\hat{\mu}_{\rm sig}$, p-value, 90% C.L. sensitivity and upper limits on the one-flavor neutrino flux normalization $\Phi_0^{90\%\rm C.L.}$ (in units of GeV^{-1} cm^{-2} s^{-1}), and on the one-flavor neutrino fluence $\mathcal{F}^{90\%\rm C.L.}$ (in units of GeV cm^{-2}), for different values of the spectral index γ. The boundaries, $E_{\rm min}$ and $E_{\rm max}$, of the energy range containing 90% of the expected signal events, employed in the calculation of the fluence, are listed in the last column.

4. Results

Figure 1 shows the distribution of the ANTARES events close to the location of the sources. In both cases, only one event has been detected within 5° from the TDE. The event close to AT2019dsg (AT2019fdr) is a track-like event, located at a distance of 1.°7 (2.°3) from the source, and was registered on 2020 February 11 (2019 September 25). The information on the two events is reported in Table 1.

The likelihood method fits less than one signal event at the direction of both TDEs for the three tested values of the spectral index $\gamma = 2.0$, $\gamma = 2.5$, and $\gamma = 3.0$. At the location of AT2019dsg, the largest deviation from the background expectation is obtained for an $E_\nu^{-3.0}$ spectrum, with a number of fitted signal events $\hat{\mu}_{\rm sig} = 0.7$ and a p-value of 8.9% corresponding to 1.3σ significance (in the one-sided convention). The lowest p-value (6.7%) at the location of AT2019fdr is observed for an $E_\nu^{-2.0}$ spectrum, with a number of fitted signal events $\hat{\mu}_{\rm sig} = 0.5$, yielding a significance of 1.5 σ (in the one-sided convention).

Table 2 summarizes the results of the searches in terms of best-fit number of signal events and p-value, and reports the

upper limits on the one-flavor neutrino flux normalization, Φ_0, for three values of γ, where the neutrino flux has been parameterized as $\Phi_\nu = \Phi_0 \left(\frac{E_\nu}{1\ \mathrm{GeV}}\right)^{-\gamma}$. Moreover, upper limits are set on the one-flavor neutrino fluence, $\mathcal{F}$, defined as the integral in time and energy of the neutrino energy flux:

$$\mathcal{F} = \int_{t_{\min}}^{t_{\max}} \int_{E_{\min}}^{E_{\max}} E_\nu \cdot \Phi_\nu \, dE_\nu \, dt = \Delta t \cdot \Phi_0 \cdot \int_{E_{\min}}^{E_{\max}} E_\nu \cdot \left(\frac{E_\nu}{1\ \mathrm{GeV}}\right)^{-\gamma} dE_\nu, \quad (3)$$

where $E_{\min}$ and $E_{\max}$ are the boundaries of the energy range containing 90% of the expected signal events for the given γ, and Δt is the live time of the search.

The absence of any significant detection of neutrinos from AT2019dsg is consistent with all proposed emission models for the TDE, with their predictions being far below the ANTARES neutrino detection threshold (Liu et al. 2020; Murase et al. 2020; Winter & Lunardini 2021). The expected neutrino fluence resulting from those models is too low to be constrained by the upper limits set in this analysis.

5. Conclusions

The ANTARES follow-up of AT2019dsg and AT2019fdr, the TDEs recently indicated as the most likely counterparts of two high-energy IceCube neutrinos, IC191001A and IC200530A, has been presented. The ANTARES data collected since the discovery of AT2019dsg and AT2019fdr have been investigated to look for a steady neutrino emission from the direction of the TDEs, resulting in no evidence for signal in the data. Given the nondetection, 90% C.L. upper limits on the one-flavor neutrino flux and fluence have been set. Recent models proposed to explain the multimessenger observations from AT2019dsg predict a neutrino emission well below the ANTARES sensitivity and cannot thus be constrained by the upper limits set in this analysis. Nevertheless, alternative search methods, such as stacking and time-dependent analyses, will provide an effective way to enhance the discovery potential using the existing data. Moreover, a significant improvement in sensitivity is expected from the upcoming next generation neutrino telescope, KM3NeT (Adrián-Martínez et al. 2016), thanks to its larger effective area combined with an excellent angular resolution (Aiello et al. 2019).

The authors acknowledge the financial support of the funding agencies: Centre National de la Recherche Scientifique (CNRS), Commissariat à l'énergie atomique et aux énergies alternatives (CEA), Commission Européenne (FEDER fund and Marie Curie Program), Institut Universitaire de France (IUF), LabEx UnivEarthS (ANR-10-LABX-0023 and ANR-18-IDEX-0001), Région Île-de-France (DIM-ACAV), Région Alsace (contrat CPER), Région Provence-Alpes-Côte d'Azur, Département du Var and Ville de La Seyne-sur-Mer, France; Bundesministerium für Bildung und Forschung (BMBF), Germany; Istituto Nazionale di Fisica Nucleare (INFN), Italy; Nederlandse organisatie voor Wetenschappelijk Onderzoek (NWO), the Netherlands; Council of the President of the Russian Federation for young scientists and leading scientific schools supporting grants, Russia; Executive Unit for Financing Higher Education, Research, Development and Innovation (UEFISCDI), Romania; Ministerio de Ciencia e Innovación (MCI) and Agencia Estatal de Investigación: Programa Estatal de Generación de Conocimiento (refs. PGC2018-096663-B-C41, -A-C42, -B-C43, -B-C44) (MCI/FEDER), Severo Ochoa Centre of Excellence and MultiDark Consolider, Junta de Andalucía (ref. SOMM17/6104/UGR and A-FQM-053-UGR18), Generalitat Valenciana: Grisolía (ref. GRISOLIA/2018/119) and GenT (ref. CIDEGENT/2018/034) programs, Spain; Ministry of Higher Education, Scientific Research and Professional Training, Morocco. We also acknowledge the technical support of Ifremer, AIM and Foselev Marine for the sea operation and the CC-IN2P3 for the computing facilities.

ORCID iDs

J. Aublin https://orcid.org/0000-0001-7642-6225
B. Baret https://orcid.org/0000-0001-6064-3858
S. Basa https://orcid.org/0000-0002-4291-333X
S. Biagi https://orcid.org/0000-0001-8598-0017
M. Bissinger https://orcid.org/0000-0002-8709-8236
S. Celli https://orcid.org/0000-0002-7592-0851
J. Hofestädt https://orcid.org/0000-0002-7848-117X
M. Kadler https://orcid.org/0000-0001-5606-6154
O. Kalekin https://orcid.org/0000-0001-6206-1288
U. Katz https://orcid.org/0000-0002-7063-4418
A. Kouchner https://orcid.org/0000-0001-7068-2113
I. Kreykenbohm https://orcid.org/0000-0001-7335-1803
R. Le Breton https://orcid.org/0000-0001-8522-4983
E. Leonora https://orcid.org/0000-0002-0536-3551
A. Margiotta https://orcid.org/0000-0001-6929-5386
A. Marinelli https://orcid.org/0000-0002-1466-1219
S. Navas https://orcid.org/0000-0003-1688-5758
C. Pellegrino https://orcid.org/0000-0002-7472-1279
P. Piattelli https://orcid.org/0000-0003-4748-6485
M. Sanguineti https://orcid.org/0000-0002-7206-2097
F. Schüssler https://orcid.org/0000-0003-1500-6571
M. Spurio https://orcid.org/0000-0002-8698-3655
Th. Stolarczyk https://orcid.org/0000-0002-0551-7581
S. J. Tingay https://orcid.org/0000-0002-8195-7562
B. Vallage https://orcid.org/0000-0003-1255-8506
J. Wilms https://orcid.org/0000-0003-2065-5410

References

Aartsen, M. G., Abraham, K., Ackermann, M., et al. 2016, ApJ, 833, 3
Aartsen, M. G., Ackermann, M., Adams, J., et al. 2014, PhRvL, 113, 101101
Aartsen, M. G., Ackermann, M., Adams, J., et al. 2018a, Sci, 361, eaat1378
Aartsen, M. G., Ackermann, M., Adams, J., et al. 2018b, Sci, 361, 147
Adrián-Martínez, S., Ageron, M., Aharonian, F., et al. 2016, JPhG, 43, 084001
Ageron, M., Aguilar, J. A., Al Samarai, I., et al. 2011, NIMPA, 656, 11
Aiello, S., Akrame, S. E., Ameli, F., et al. 2019, APh, 111, 100
Albert, A., Alves, S., André, M., et al. 2021, PhLB, 816, 136228
Albert, A., André, M., Anghinolfi, M., et al. 2017, PhRvD, 96, 082001
Albert, A., André, M., Anghinolfi, M., et al. 2018a, ApJL, 853, L7
Albert, A., André, M., Anghinolfi, M., et al. 2018b, ApJL, 863, L30
Barr, G. D., Gaisser, T. K., Lipari, P., Robbins, S., & Stanev, T. 2004, PhRvD, 70, 023006
Bellm, E. C., Kulkarni, S. R., Graham, M. J., et al. 2018, PASP, 131, 018002
Biehl, D., Boncioli, D., Lunardini, C., & Winter, W. 2018, NatSR, 8, 10828
Frederick, S., Gezari, S., Graham, M. J., et al. 2020, arXiv:2010.08554
Graham, M. J., Kulkarni, S. R., Bellm, E. C., et al. 2019, PASP, 131, 078001
Komossa, S. 2015, JHEAp, 7, 148
Kopper, C., & Blaufuss, E. 2017, GCN Circ. 21916
Liu, R.-Y., Xi, S.-Q., & Wang, X.-Y. 2020, PhRvD, 102, 083028
Lodato, G., Franchini, A., Bonnerot, C., & Rossi, E. M. 2015, JHEAp, 7, 158
Murase, K., Kimura, S. S., Zhang, B. T., Oikonomou, F., & Petropoulou, M. 2020, ApJ, 902, 108
Nordin, J., Brinnel, V., Giomi, M., et al. 2019, TNSTR, 615, 1

Reusch, S. 2020, GCN Circ. 27872
Stein, R. 2019, GCN Circ. 25913
Stein, R. 2020a, ICRC (Madison, WI), 1016
Stein, R. 2020b, GCN Circ. 27865
Stein, R., van Velzen, S., Kowalski, M., et al. 2021, NatAs, 5, 510
Winter, W., & Lunardini, C. 2021, NatAs, 5, 472